Prevalence and origin of birefringence in 48 garnets from the pyrope-almandine-grossularite-spessartine quaternary

ANNE M. HOFMEISTER,[1,*] RAND B. SCHAAL,[2] KARLA R. CAMPBELL,[2] SANDRA L. BERRY,[2] AND TIMOTHY J. FAGAN[2]

[1]Department of Earth and Planetary Sciences, Washington University, St. Louis, Missouri 63130, U.S.A.
[2]Department of Geology, University of California, Davis, California 95616, U.S.A.

ABSTRACT

Forty garnets are anisotropic among 48 in a suite spanning the quaternary system $Mg_3Al_2Si_3O_{12}$-$Fe_3Al_2Si_3O_{12}$-$Ca_3Al_2Si_3O_{12}$-$Mn_3Al_2Si_3O_{12}$ (Py-Al-Gr-Sp). The eight isotropic specimens are too thin (<0.4 mm) for detection of weak anisotropy. Birefringence (δ) in the remaining 40 garnets is low (δ = 0.0001 to 0.0006) and undulatory in appearance, suggesting that most optical anomalies in quaternary garnets, including the pyrope-almandine-spessartine ternary, originate through residual strain. Multiple or alternate origins are not precluded for the few samples with nearly uniform retardation or unusual sector twinning. An inverse correlation exists between degree of birefringence and stresses encountered during tectonic deformation. That is, mantle garnets from kimberlites (e.g., $Py_{37}Al_{36}Gr_{27}$) have the highest δ values. As geologic setting is difficult to separate from composition, the inverse trend suggests that birefringence arises partially from internal factors. We propose that the mismatch in size between Ca^{2+} and Mg^{2+} exacerbates retention of residual strain. Short-range ordering is not entirely ruled out, but clustering has only been inferred for synthetics in the middle of the Py-Gr binary, a composition range unknown for natural samples, and domains are precluded in the natural samples by the recent X-ray studies of samples from similar localities.

INTRODUCTION

Biaxial optical properties in nominally uniaxial minerals, such as quartz, or in nominally isotropic minerals, such as diamond, are generally attributed to strain induced externally by tectonic deformation of the host rock. However, birefringence commonly observed in garnets within the solid-solution series between grossularite (Gr = $Ca_3Al_2Si_3O_{12}$) and andradite (An = $Ca_3Fe_2Si_3O_{12}$) has been attributed to factors of crystal chemistry, such as partial cation ordering (see reviews by Meagher 1982 and Griffen 1992), instead of deformation. Birefringence exists in garnets of a wide range of compositions (see summary by Deer et al. 1982), including uvarovites (Uv = $Ca_3Cr_2Si_3O_{12}$) (Foord and Mills 1978), spessartines (Sp = $Mn_3Al_2Si_3O_{12}$) (Smyth et al. 1990), and diverse synthetic garnets (Kitamura and Komatsu 1978; Chase and Lefever 1960). However, crystallographic refinements of more than 280 samples (Merli et al. 1995; see also Armbruster and Geiger 1993) show no evidence of symmetry reduction. Birefringence has been reported in a few quaternary garnets [Gr-pyrope (Py = $Mg_3Al_2Si_3O_{12}$)-almandine (Al = $Fe_3Al_2Si_3O_{12}$) garnet with minor spessartine components] (Kano and Yashima 1976; Griffen et al. 1992; Brown and Mason 1994), although these compositions and pyralspites are commonly assumed to be cubic. (The name pyralspite is used as a convenient abbreviation here for garnet solid solutions within the Py-Al-Sp ternary.) The primary purpose of this study is to draw attention to the ubiquitous occurrence of weak and undulatory birefringence throughout a large suite of pyralspites and quaternary garnets. Origins of birefringence are discussed in view of our new data and recent structural (Rossmanith and Armbruster 1995; Quartieri et al. 1995; Ungaretti et al. 1995) and spectroscopic (Bosenick et al. 1995; McAloon and Hofmeister 1995; Hofmeister et al. 1996) studies, particularly the likelihood of strain.

EXPERIMENTAL METHODS

We acquired 48 single-crystal garnets strictly on the basis of composition, in an effort to span the Gr-Py-Al ternary with minimal An, Uv, or Sp components (Table 1), with an emphasis on large size (>0.5 mm) to obtain high-quality infrared (IR) spectra. The specimens were not selected on the basis of optical properties. It was the surprising prevalence of anisotropy that spawned the present study.

Crystals were polished and examined with a petrographic microscope. Optical retardation (Δ) was estimated visually by comparison with a Michel-Lévy interference color chart. The variable and undulatory nature of retardation made the attempt of obtaining a precise quantitative measurement of retardation with a Berek compen-

* E-mail: hofmeist@levee.wustl.edu

TABLE 1. Sample characteristics

Index no.	Polish*	Retar-dation (nm)	Thickness (mm)	Diameter (mm)	Birefrin-gence	Composition Py-Al-Gr-Sp-Uv-An	Rock type/Host occurrence
1	D	100	0.542	4.0	0.0002	71-18-3-1-3-4†	eclogite xenolith
2	D	200	0.460	2.0	0.0004	0-0.5-99.5-0-0-1†	GR vein in serpentinite
3‡	D	150	0.729	4.0	0.0002	95-4-2-0-0-0§	garnet blueschist
4	D	150	0.520	4.0	0.0003	68-18-2-1-11-0†	xenocryst in ultramafic dike
5	N	50	2.351	4.0	<0.0001	71-15-12-0-2-0	xenocryst in ultramafic dike
6	D	100	0.731	2.0	0.0001	67-20-3-1-9-0	xenocryst in ultramafic dike
7	D	150	0.793	3.0	0.0002	59-33-7-1-0-0§	xenocryst in ultramafic dike
8	D	200	0.859	4.0	0.0002	67-20-7-1-5-0†	xenocryst in ultramafic dike
9	D	200	0.618	3.0	0.0003	67-25-7-0-0-0§	xenocryst in ultramafic dike
10	D	50	0.172	1.5	0.0003	47-40-13-0-0-0†	eclogite xenolith
11	D	?	0.127	1.0	isotropic	18-78-4-0-0-0§	schist
12	D	?	0.028	1.0	isotropic	31-38-30-1-0-0†	kyanite eclogite xenolith
13	D	150	0.270	2.0	0.0006	72-18-3-1-3-4	eclogite xenolith
14	S	100	0.529	1.0	0.0002	52-20-22-1-2-4	eclogite xenolith
15	S	?	0.042	0.5	isotropic	28-24-47-1-0-0†	coesite grospydite xenolith
16	D	150	0.430	2.5	0.0003	41-45-13-1-0-0†	porphyroblasts in gabbro
17	D	125	1.050	4.0	0.0001	10-73-3-14-0-0§	schist
18	D	90	0.150	1.0	0.0006	72-17-6-1-1-3‖§	Group II eclogite xenolith
19	D	100	0.197	1.0	0.0006	18-17-62-0-0-3‖†	Group I eclogite xenolith
20	S	100	0.270	1.0	0.0003	54-35-4-1-1-5‖§	Group I eclogite xenolith
21	D	?	<0.040	1.0	isotropic	58-19-23-0-0-0‖	Group I eclogite xenolith
22	D	100	0.269	1.0	0.0004	55-29-13-1-0-2‖	Group I eclogite xenolith
23	D	100	0.219	1.0	0.0004	37-35-24-1-0-3‖†	Group I eclogite xenolith
24	D	120	1.326	3.0	<0.0001	3.5-65-0.5-31-0-0	pegmatite
25	S	100	1.446	6.0	<0.0001	3-25-28-31-0-13	pegmatite
26	S	100	0.891	2.5	0.0001	1-20-24-35-0-19	aplite
27	S	?	1.699	3.0	opaque	4-46-26-24-0-00	schist
28	D	150	1.652	7.0	<0.0001	assumed same as no. 17	schist
29	D	100	1.139	3.0	<0.0001	15-61-20-4-0-0†	felsic volcanic
30‡	D	200	1.635	4.0	0.0001	8-80-2-9-0-0§	peletic schist
31	N	50	0.189	2.0	0.0003	71-16-5-1-1-6‖	garnet-illmenite nodule
32	D	200	0.795	2.0	0.0003	36-21-42-0-0-1	grospydite xenolith
33	D	100	0.424	1.0	0.0002#	44-48-6-2-0-0§	hornfels
34‡	D	250	1.137	2.0	0.0002	40-50-7-3-0-0§	hornfels
35‡	D	100	0.863	7.0	0.0001	2-58-0-39-0-0	aplite
36	D	120	0.974	8.0	0.0001	43-54-2-1-0-0	unknown
37	D	120	0.684	5.0	0.0002	assumed same as no. 40	qtz-mica-grt schist
38‡	D	100	1.681	3.0	<0.0001**	6-86-6-2-0-0§	schist
39	D	100	1.558	9.0	<0.0001	1-61-1-37-0-0	unknown
40‡	D	200	0.963	5.0	0.0002#	58-37-3-2-0-0§	qtz-mica-grt schist
41	D	?	0.356	0.0	isotropic	0-100-0-0-0-0‖§	synthetic almandine
42	D	50	1.065	1.5	<0.0001	6-50-33-10-0-0‖	tonalite
43	N	?	0.654	0.0	isotropic	54-41-5-0-0-0‖§	synthetic polycrystal
44	N	200?	1.000	1.5	0.0002	5-0-88-0-0-7‖	vesuvianite skarn
45	D	?	0.253	0.3	isotropic	4-39-48-2-0-7†	qtz-feldspar-grt granulite
46	D	100	0.788	2.0	0.0001	20-74-3-3-0-0	sillimanite gneiss
47	D	100	0.631	12.0	0.0002	5-72-17-3-0-3	granite
48	S	?	0.200	1?	isotropic	1.4-2.4-1-95-0-0‖	pegmatite

Note: Uncertainties are in the last digit, except for retardation which is ±50.
* D = doubly polished; S = singly polished; N = not polished.
† Microprobe analysis and IR spectra in Hofmeister et al. (in preparation).
‡ Section shown in Figure 1.
§ Microprobe analysis and IR spectra in Hofmeister et al. (1996).
‖ Microprobe analysis taken from the literature cited in the reference column.
These two samples had nearly uniform extinction, all others were wavy, undulatory, or spotty.
** Weak, sectored retardation.

sator (or from oriented samples) ineffectual. However, the differences among the samples are real, albeit small, because measurements of duplicate samples or several fragments from one crystal yielded the same values for δ, and because samples were compared side by side in the microscope to secure consistent results. Essentially the sam-

ples were ordered in retardation. Measured retardation was found to be independent of thickness, which suggests that optical activity cannot be the cause, and consistent with the space group of cubic garnet possessing a center of inversion (Bloss 1971). Birefringence (δ) was calculated from

TABLE 1—*Extended*

Location	Donor	Sample No.	Reference
Frank Smith Mine, South Africa	R.M. Hazen, J.R. Smyth	SFS4	Boyd (1974)
Georgetown, California	R.M. Hazen, J.R. Smyth		Pabst (1936)
Dora Maria Massif, Italy	R.M. Hazen, J.R. Smyth	SDM-1	Chopin (1984)
East Garnet Ridge Dike, Arizona	R.B. Schaal	EGR-1X	Schaal (1991)
East Garnet Ridge Dike, Arizona	R.B. Schaal	EGR-4X	Schaal (1991)
Moses Rock Dike (anthill), Utah	R.B. Schaal	MOS-1X	Schaal (1991)
Moses Rock Dike, Utah	R.B. Schaal	MOS-2X	Schaal (1991)
Moses Rock Dike (anthill), Utah	R.B. Schaal	MOS-3X	Schaal (1991)
Moses Rock Dike, Utah	R.B. Schaal	MOS-4X	Schaal (1991)
Bobbejaan Kimberlite, South Africa	R.M. Hazen, J.R. Smyth	SBB23	
Emerald Creek, Latah Co., Idaho	R.M. Hazen, J.R. Smyth	NMNH 107105	Novak and Gibbs (1971); Hietanen (1963)
Bobbejaan Kimberlite, South Africa	R.M. Hazen, J.R. Smyth	SBB1	Smyth and Hatton (1977)
Frank Smith Mine, South Africa	R.M. Hazen, J.R. Smyth	SFS4	Boyd (1974)
Roberts Victor Kimberlite, South Africa	R.M. Hazen, J.R. Smyth	SRV4	Caporscio and Smyth (1990)
Roberts Victor Kimberlite, South Africa	R.M. Hazen, J.R. Smyth	SRV1	O'Neill et al. (1989); Smith and Hatton (1977)
Gore Mountain, Essex Co., NY	UCD Museum	SM1348	Levin (1950); Deer et al. (1982, p. 503, no. 26)
Fort Wrangell, Alaska	UCD Museum	SM1090	Pabst (1943)
Roberts Victor Kimberlite, South Africa	UCD Museum	R-8A	MacGregor and Manton (1986)
Roberts Victor Kimberlite, South Africa	UCD Museum	R-53	MacGregor and Manton (1986)
Roberts Victor Kimberlite, South Africa	UCD Museum	R-71a	MacGregor and Manton (1986)
Roberts Victor Kimberlite, South Africa	UCD Museum	R-56	MacGregor and Manton (1986)
Roberts Victor Kimberlite, South Africa	UCD Museum	R-16	MacGregor and Manton (1986)
Roberts Victor Kimberlite, South Africa	UCD Museum	R-36	MacGregor and Manton (1986)
unknown	T.J. Fagan		
unknown	A.A. Finnerty III		
unknown	A.A. Finnerty III		
Chowchilla River, California, Buchanan Mine	P. Gennaro		
Fort Wrangell, Alaska	P. Gennaro	UCB 12606	Pabst (1943)
Salmon River, California	T.J. Fagan		
Mt. Monadnock, New Hampshire	T.J. Fagan		Thompson (1985)
Excelsior Kimberlite, South Africa	F.R. Boyd	1824/6	Boyd and Dawson (1972)
Zagadochnaya Kimberlite, Yakutia, Siberia	F.R. Boyd	Z7	Sobolyev (1966); Deer et al. (1982, p. 503, no. 28)
De Luca Pit, Emery Hill, Cortlandt, NY	F. Barker		Barker (1964)
Emery Hill, Cortlandt, NY	F. Barker		Barker (1964)
Valenca Minho, Portugal	W.C. Metropolis	Harvard 104623	
unknown	W.C. Metropolis	Harvard 129076	
Cowee Valley, N. Carolina	W.C. Metropolis	Harvard 118502	Deer et al. (1982, p. 501, no. 16)
Harney Peak Dist., S. Dakota	W.C. Metropolis	Harvard 102872	
Yamano Province, Japan	W.C. Metropolis	Harvard 34983	
Macon Co., N. Carolina	UCD Museum	SM 1597	Deer et al. (1982, p. 501, no. 16)
	S.R. Bohlen	synalm	UCD Probe lab standard
Bushy Point, Alaska	J. Hammarstrom	82-7-5	Zen and Hammarstrom (1988)
	A.M. Koziol	AK 51	Koziol and Newton (1989)
Xalostoc, Morelos, Mexico	UCD Museum	Sm1602	Prandl (1966)
Big Creek, California	S. Sorensen	NMNH 116478-15	Dodge et al. (1988) B37
Big Creek, California	S. Sorensen	NMNH 116478-26	Dodge et al. (1988) B60
Potato Hill Pluton, Newfoundland	J.V. Owen	VO-87-041A	Owen and Marr (1990)
Minas Geras, Brazil	G.R. Rossman	GRR-12372	Hofmeister and Chopelas (1991)

$$\delta = N - n = \Delta/t \qquad (1)$$

(e.g., Kerr 1977), where N is the greater index of refraction, n is the lesser, and t is the thickness (in nanometers). Thickness and diameter were measured with a digital micrometer or by comparison with a calibrated microscope reticle. Chemical compositions were obtained with a Cameca SX-50 electron microprobe at the University of California, Davis. Analytical methods are given by Hofmeister et al. (1996). Several spots between cores and rims were selected for analysis, and chemical zoning was not detected. Duplicate samples, numbers 28 and 37, were not analyzed.

RESULTS

Optical birefringence is common in the suite of 48 garnets (Table 1) and extinction is generally undulatory. One almandine (no. 38, Fig. 1e) resembles the sample described by Brown and Mason (1994) but has poorly developed sector twinning. Only garnets numbers 34 and 40 exhibit extinction that approaches uniformity (Fig. 1). The uniformity may not be a significant difference because number 17, which is from the same locality as number 40, has wavy extinction. Most samples contain bands or spots of high retardation. Retardation is typically highest near inclusions or fractures, if present (Fig. 1f). Halos
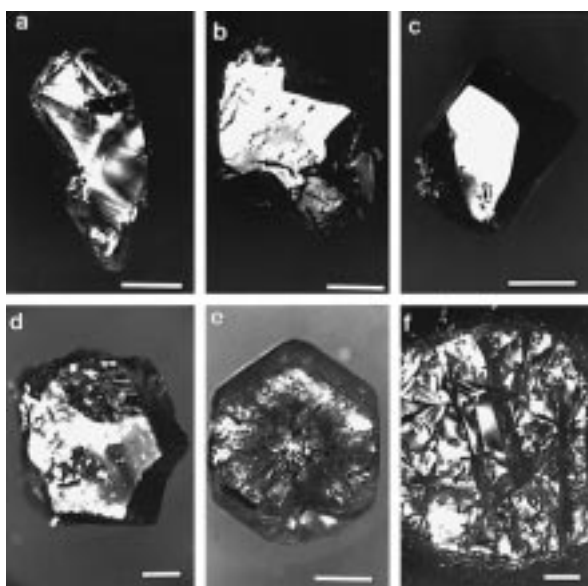
FIGURE 1. Photomicrographs taken with crossed polarizers of representative and unusual garnets. (**a**) Typical undulatory extinction in near end-member pyrope (no. 3). (**b**) Unusual uniform birefringence in a Py-Al binary (no. 40). (**c**) Unusual uniform extinction in almandine (no. 34). (**d**) Typical wavy extinction in a Ca-rich almandine (no. 30). (**e**) Atypical weakly sectored Ca-rich almandine (no. 38). (**f**) Typical spotty birefringence in Al-Sp binary (no. 35). All samples are doubly polished. None has detectable Uv or An components. Scale bars are 1 mm.

FIGURE 2. Dependence of birefringence on the diameter of the crystal (**a**) and its thickness (**b**). Filled symbols have mantle origins, see also Table 1. The lines and arrows indicate the minimum thickness for which given values of birefringence can be observed. High *T,* low *P* rocks include granites, gabbros, hornfels, and pegmatites. Sample number 16 has a composition similar to those of the mantle samples. Sample number 2 is nearly pure grossularite, and may have a different origin for its birefringence.

are commonly observed around inclusions. However, the extinction for the sample in Figure 1b is nearly uniform, despite the presence of inclusions, and wavy or spotty extinction occurs in regions of other samples without cracks or inclusions (Figs. 1a and 1d). These irregularities preclude accurate determination of the orientation of optic axes and 2V angles. Given the irregular nature of the retardation, neither did it seem worthwhile to orient the samples. Thus, the values listed in Table 1 represent not the true birefringence but an apparent and approximate birefringence.

Only eight samples appear isotropic (including both synthetic garnets, numbers 41 and 43), whereas 26 garnets are marginally birefringent ($\delta \leq 0.0002$), and 13 garnets have low birefringence ($\delta = 0.0003$ to 0.0006). Retardation could not be estimated for sample number 27 because it was rendered opaque by a high density of inclusions.

Cutting or polishing did not induce retardation because this phenomenon was observed in crystal fragments. It is unlikely that the birefringence was caused by inclusions because these are not present in all samples. [For further discussion of this point, see Brown and Mason (1994).]

Relationships between optical properties and crystal size

Birefringence correlates poorly with the diameter of garnet crystals (Fig. 2a). For the 40 samples with diameter below 4 mm, δ occupies the full range and its values
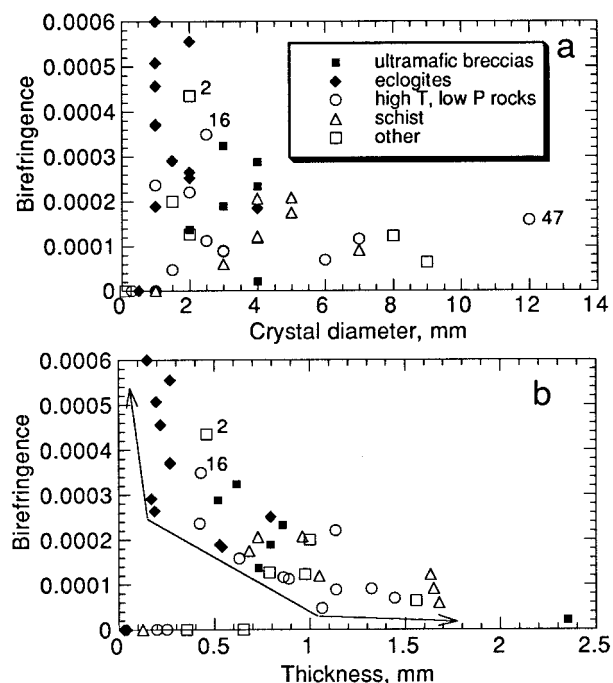
are evenly distributed in this thickness range. For the eight samples above 4 mm, only low values are seen, but this distribution appears to be correlated with geologic setting or chemical composition (the largest samples are of crustal origin and poor in Ca and Mg, whereas the smaller samples are from mantle and rich in Ca and Mg), discussed below.

A minimum thickness is needed to create a sufficient path difference to measure retardation for a particular δ (Eq. 1). For example, in garnets with δ as low as 0.0002, Δ can be determined only in relatively thick samples ($t \geq 0.4$ mm). However, in garnets with $\delta \geq 0.0003$, Δ can be determined in thinner samples ($t \geq 0.17$ mm). The requirement of a minimum thickness for a given δ partially causes the inverse correlation of Figure 2b, in that samples that should fall within the lower right corner are restricted artificially to the *x* axis. That is, sample numbers 41, 43, 45, and 48, that are listed as isotropic, with $t \geq 0.2$ mm, could actually have δ as high as 0.0002. The other four isotropic samples (nos. 11, 12, 15, 21) are all thin ($t < 0.13$ mm) and could actually have even higher δ. Thus, all 48 garnets could be weakly anisotropic. Isotropic garnets are not considered further in this study be-
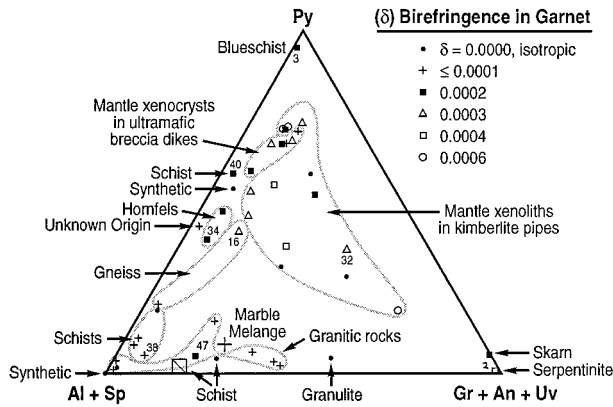
FIGURE 3. Psuedo-ternary plot of chemical composition that indicates degree of average birefringence. Large plus sign, Ca-rich almandine of Griffen et al (1992). Large square with slash, sectored almandine of Brown and Mason (1994). Other symbols are described in the legend. Labels indicate host rock types. Enclosed areas link garnets of common origin. "Granitic" host rocks include granite, tonalite, aplite, felsic volcanic, and pegmatite.

cause all of these specimens (Table 1) are too small to detect retardation.

The weak correlation of relatively large values of birefringence with thin samples appears to result from geologic setting or chemical composition. The mantle samples, which are rich in both Ca and Mg, are thin (because they are smaller), and this subset apparently has the highest values of δ (see below).

The generally small size of synthetic crystals and the use of thin sections (~0.030 mm) for petrographic study of natural samples precludes detection of birefringence in most garnets. For example, Ganguly et al. (1993) lists crystal sizes of 0.015 to 0.060 mm for synthetic pyrope-grossularite solid solutions. The birefringence of these synthetic Py-Gr garnets and of natural samples in thin section would need to be an order of magnitude larger than that observed here for detection. Hence, it is not surprising that ubiquitous birefringence in pyralspite garnets has previously gone unreported.

Relationship between birefringence and chemical composition

All but three of the specimens analyzed in this study contain ≥86 mol% Py+Al+Gr. Thus, although the compositions should technically be described in terms of six components, the suite can be approximated by the pseudo-ternary system Py-Al-Gr (Fig. 3). Those three exceptions are number 35, with 39 mol% Sp, number 39, with 37 mol% Sp, and number 24, with 31 mol% Sp, although representation of number 25, with 13 mol% An, and number 26, with 19 mol% Sp, are also not ideal. However, the optical properties of these samples resemble those of garnets that are well-described by the ternary. This suite allows examination of possible relationships between birefringence and amounts of Ca, Mg, and Fe in garnets.

Garnets from each sub-region of the pseudo-ternary diagram (Fig. 3; Table 1) exhibit birefringence, including near end-member compositions (nos. 2, 3, and 38), binary Py-Al garnets (nos. 34 and 40), binary Al-Sp garnets (nos. 35 and 39), near binary Al-Gr garnets (nos. 38 and 47), pyralspites (Py-Al-Sp) with minor Gr-components (nos. 17 and 30), and quaternary garnets (Gr-Py-Al) with minor Sp-components (nos. 16 and 32). Data are absent between the Py-corner and the (Gr+An+Uv)-corner and also for very Fe-rich grossularites (Fig. 3) because natural garnets of those compositions apparently do not exist (see also Ungaretti et al. 1995). Synthetic samples (e.g., Py-Gr garnets) were not sought because the grain size is too small to detect low birefringence (or for single-crystal IR study, our original purpose).

Generally, the highest values of birefringence (δ = 0.0003 to 0.0006) are found in quaternary Py-Al-Gr garnets (center of Fig. 3). Intermediate values (δ ≤ 0.0002) occur in near-binary Py-Al solid solutions with <10 mol% Gr and <60% Al (upper left edge of the triangle in Fig. 2); and the lowest values are found in almandines (lower left corner of Fig. 3). The only exceptions to the pattern are the sectored almandine of Brown and Mason (1994) and near end-member grossularite; however, the birefringence of these samples may have a different origin (see discussion section). This pattern suggests that birefringence correlates positively with Ca^{2+} coexisting with Mg^{2+}. The correlation is weak, however, partially due to the difficulty in quantifying the irregular birefringence of these samples. No other major elements (e.g., Fe^{3+} or Cr^{3+}) were found to correlate with δ. Trace element contents were not measured because the existing literature on mantle samples (e.g., MacGregor and Manton 1986) did not suggest any positive correlations (see also the discussion section).

Relationship between birefringence and geologic setting

Garnet compositions vary with the type of host rock and with geologic setting (enclosed areas of Fig. 3). Garnets from the upper mantle generally lie inside the Py-Al-Gr psuedo-ternary (Fig. 3), whereas garnets from crustal metamorphic and igneous rocks generally fall in either the pyralspite or grandite solid solutions (see summary by Deer et al. 1982). Thus, the correlation of birefringence with chemical composition could actually result from conditions of formation, subsequent pressure-temperature path, and possible externally applied stresses. Specifically, the highest birefringence occurs in mantle xenocrysts from ultramafic breccia dikes in the Colorado Plateau and in garnets within eclogite xenoliths found in kimberlites from southern Africa or Siberia (Fig. 2). Not only did these garnets crystallize at the highest pressures and are thus the farthest from their conditions of formation, but the rapid decompression would promote retention of whatever strain features occurred during growth. In contrast, strain in crustal garnets would have been annealed away as these cooled more slowly (R.F. Dymek, personal communication).

Evidence against geologic setting and in favor of composition as the primary factor controlling birefringence are that: (1) the eclogitic garnet of Griffen et al. (1992), which was reworked in an ophiolite, has low $\delta = 0.0002$ like that of other almandines, despite the high stresses encountered; and (2) a Ca-rich pyralspite from crustal rocks (no. 16) has both composition and birefringence similar to that of mantle garnets (Figs. 2 and 3). The almandine of Brown and Mason (1994) has an unusually high δ compared to garnets of similar composition and similar geologic setting. This sample is strongly sectored, unlike the weak sectoring seen in one almandine here, which may indicate a different mechanism for the origin of its optical anomalies.

ORIGIN OF BIREFRINGENCE IN GARNET

Previous models

Birefringence previously observed in solid solutions of Gr-An-Uv (abbreviated as ugrandite) and in Sp-rich garnets is highly variable and can be two orders of magnitude larger than that in pyralspites and quaternary garnets (Table 1), suggesting different origins. For example, $Sp_{87}Al_{11}Gr_2$ with 3.7 wt% F and 0.6 wt% H_2O has $\delta = 0.008$ (Smyth et al. 1990); An-garnets have $\delta = 0.005$ (Kingma and Downs 1989); and Gr-An garnets can have $\delta = 0.010$ (Foord and Mills 1978). We do not address the origin of such "large" optical anomalies because the causes may be diverse and unrelated. Only weak anomalies are discussed here: This study focuses on whether any of five reported hypotheses for anisotropy in garnet, summarized by Kingma and Downs (1989), can explain the prevalent and variable birefringence observed in our suite of 48 pyralspites and quaternary garnets. However, unique causes of birefringence for a few of our samples (e.g., 32, 38, and 40) are not precluded.

(1) *Large scale twinning* (Ingerson and Barksdale 1943) cannot be important, because twinning is visible in only one sample (no. 38) from the suite examined in this study and is reported in only one other almandine (Brown and Mason 1994) of similar composition and geologic setting. However for this sectored almandine, twinning and compositional zoning are not directly linked with the birefringence, as discussed by Brown and Mason (1994). In contrast, twinning has been connected with the sector zoning seen in grossularite-andradites (Allen and Buseck 1988; Akizuki 1984). For the zoned ugrandites, birefringence was interpreted as a result of varying degrees of Fe^{3+}/Al ordering produced on the side faces of surfaces during growth (Akizuki 1984). This type of ordering could be short- or long-range. Problems with ordering as the cause of birefringence are discussed under point (4).

Sub-optical twins could be present, although such has not been detected in crystallographic studies (e.g., Prandl 1966; Novak and Gibbs 1971; Allen and Buseck 1988; Smyth et al. 1990; Griffen et al. 1992; Merli et al. 1995). However, disproving the existence of such twins requires electron microscopy because form birefringence has been observed in magnetites, originating from zones as small as 100 nm (Libowitzky 1995).

(2) *Non-cubic distribution of OH^--groups* (Rossman and Aines 1986) is unlikely, because pyralspites typically contain less than 0.25 wt% H_2O (Aines and Rossman 1984). Some of our birefringent garnets contain no detectable water even in cm-thick single-crystals (Schaal et al., in preparation).

(3) *Effects of undetected trace elements,* such as magneto-optic effects from rare-earth elements (REE) substituting for calcium (Blanc and Maisonneuve 1973), are deemed unlikely, given the wide variety of compositions of anisotropic garnets, their diverse host rocks, and their distinct geological settings. Furthermore, synthetic garnets that contain stoichiometric REE (e.g., $Y_3Fe_5O_{12}$) develop only weak birefringence.

(4) *Reduction of symmetry by partial long-range ordering of Ca^{2+} and Fe^{2+} in distorted dodecahedral sites* has been suggested as a cause of birefringence on the basis of crystallographic refinement of a Ca-rich almandine (Griffen et al. 1992) and of two grossularites (Allen and Buseck 1988). In contrast, $Ia\overline{3}d$ structures were obtained from crystallographic study of other birefringent quaternary garnets [spessartine (Smyth et al. 1990)], and for garnets from the same localities as ours and presumably with similar birefringence [grossularite no. 44, which was investigated by neutron scattering (Prandl 1966); pyrope number 3, which was investigated by inelastic neutron scattering (Artioli et al. 1996); and X-ray diffraction (XRD) of 281 samples, including four from the same localities as numbers 3, 10, 32, and 48 (Merli et al. 1995; Quartieri et al. 1995; Ungaretti et al. 1995)]. Isotropic samples were specifically sought by the Pavia consortium, and at the thicknesses of 0.3 to 0.8 mm examined under crossed polars, distinct retardation was not seen, although some samples had imperfect extinction, e.g., garnet from the Zadochnaya kimberlite (M. Merli, personal communication 1997). Thus at least a few of the 281 samples examined were birefringent. Also, synthetic Gr-Py solid solutions possess the cubic $Ia\overline{3}d$ structure (e.g., Ganguly et al. 1993). Elasticity measurements of chemically diverse garnets, including mantle samples similar to numbers 15 and 22 from this study are consistent with cubic symmetry (e.g., O'Neill et al. 1989; Chai and Brown 1997). Furthermore, single-crystal IR spectra of the samples in Table 1 are consistent with a cubic space group (Hofmeister et al. 1996; in preparation).

The discrepancies among the crystallographic studies, and the disagreement of these with spectroscopic measurements, can be attributed to the similar scattering powers of Ca, Mg, and Fe, which makes it impossible to prove (or disprove) long-range ordering (Rossmanith and Armbruster 1995; Armbruster, personal communication).

Short-range ordering (Bosenick et al. 1995) has been detected in synthetic samples from the middle of the Gr-Py binary through nuclear magnetic resonance (NMR), but not for the end-members. This result does not contradict the above crystallographic study because not only are

the compositional ranges different, but moreover the NMR sampling scale is extremely small (nearest and next-nearest neighbors) compared to XRD (~100 unit cells), and hence clustering detected by NMR need not be resolved by XRD methods.

(5) *Strain* (Chase and Lefever 1960; Lessing and Standish 1973; Kitamura and Komatsu 1978) appears to be a primary cause of optical anisotropy in pyralspites and quaternary garnets. Low birefringence and undulatory extinction occurring in our suite of 48 garnets support this hypothesis. Strain may account for inconsistent interpretations of space groups, as revealed in some crystallographic studies and spectroscopic studies, because XRD requires a large contiguous volume (~100 unit cells) and would be affected by strain, whereas IR spectra are derived on the scale of a unit cell. Furthermore, powder XRD data from birefringent garnets have patterns indicative of the cubic structure (Kingma, personal communication), consistent with strain rather than ordering. The selection of nearly isotropic samples by the Pavia consortium minimizes strain, yielding diffractions consistent with an $Ia\overline{3}d$ space group.

Interpretation

Hypotheses 1 through 4, above, are discounted as the origin of prevalent birefringence in the psuedo-ternary, because the 48 garnets that we examined do not exhibit the features described in those models. Our observations of wavy, low birefringence for many samples with varying composition support hypothesis 5. We favor a mainly internal origin for the strain, as follows.

If a deviatoric stress is applied to a crystal during or after crystallization, then strain may be preserved and be exhibited as retardation. In our suite, a positive correlation does not exist between the type of deformation typical of each geologic setting and the strength of birefringence in garnets from it. Instead, the inverse holds. Mantle xenocrysts found in ultramafic breccia dikes from Arizona and Utah exhibit birefringence although they traveled undeformed and unaltered through the Earth's crust in a lapsed time estimated to be hours (McGetchin et al. 1973), while suspended within a low-temperature, volatile-charged aqueous slurry (McGetchin and Silver 1970, 1972). Likewise, eclogite xenoliths found in diamondiferous kimberlite pipes contain birefringent garnets, but they also arrived at the surface with unfractured, undeformed cumulate (Group I eclogites) and granoblastic (Group II eclogites) textures (MacGregor and Carter 1970). On the other hand, deformed, strongly foliated metamorphic rocks have the highest likelihood of encountering post-crystallization strain, but garnets in schists and gneisses in our suite have the lowest values of birefringence. Igneous garnets may or may not retain strain, depending on timing of crystallization and on the extent of deformation during uplift, but those in this study also have weak birefringence. Externally derived stresses cannot be the sole source of birefringence in garnets, although deformation of the host rock undoubtedly introduces some strain that, if not relaxed, adds to the anisotropy.

Compositional dependence of birefringence in quaternary garnets that cuts across geologic setting (Figs. 2 and 3) suggests an internal origin for the strain, specifically, the mismatch in size between Ca^{2+} and Mg^{2+} in the distorted dodecahedral site. Two facts pertain: (1) positive excess volumes of mixing, with ~0.5% as the maximum are seen for the for Py-Gr join, mainly due to the increased size of the dodecahedron with increasing Ca substitution (e.g., Ungaretti et al. 1995; Ganguly et al. 1993); and (2) anisotropic, dynamic displacement exists for Ca^{2+} in andradite (Armbruster and Geiger 1993), but is less than the "rattling effects" of Mg^{2+} in pyrope or of Fe^{2+} in almandine (Armbruster et al. 1992). We hypothesize that internal strain may arise from non-random spatial distributions of X-site disorder. As the Ca-content increases, the dodecahedron expands, and the magnitude of dynamic disorder for Mg^{2+} in the X-site probably increases. In this model, preferential orientations for site disorder are created by the specific distribution of defects within the crystal (e.g., the Mg cations on both sides of a plane or line dislocation move away from the dislocation) and anisotropy of the dynamic disorder on X-sites cause the optical anisotropy. The wavy, spotty, or undulatory patterns occur because the dynamic site disorder switches orientation as various defects are encountered (e.g., grain boundaries) such that the crystal structure is cubic, on average. This internally derived strain may be augmented or exacerbated by tectonic stresses. Alternatively, there could be a component of short-range ordering in these garnets on a scale resolvable by NMR, but not by X-ray, absorption, or scattering methods. The question in this case is whether clustering could produce optical anomalies on the mm scale observed here.

For ugrandite garnets, the ubiquitious occurrence of optical anolamies is well documented (e.g., Meagher 1982). For example, all garnets in the suite of 51 collected for IR study (McAloon and Hofmeister 1995) were found to be birefringent to some degree. Thus, is it certain that the $Ia\overline{3}d$ samples examined by the Pavia group contained ugrandites with weak retardation, although strongly birefringent samples were excluded from their crystallographic determinations, given the specific selection criteria (Merli et al. 1995). Crystallographic study of birefringent andradite garnet similarly yielded the cubic structure and, more importantly, the amount of strain was not reduced if a triclinic space group was used for the refinement (Armbruster and Geiger 1993). Ugrandite garnets with low amounts of birefringence are inferred to be strained, similar to the pyralspitic garnets, and crystallographic determinations of partial ordering of such samples may be adversely affected by the presence of strain (see McAloon and Hofmeister 1993). For this solid solution, we hypothesize that the internal strain primarily arises in structural variations of the tetrahedral site, derived from its unusually long bond lengths and irregular shape. Thus, the hydrogarnet substition in the tetrahedra

could play a crucial role or it simply could be a passive marker of the distortions.

ACKNOWLEDGMENTS

REFERENCES CITED

Aines, R.D. and Rossman, G.R. (1984) The hydrous component in garnets: pyralspites. American Mineralogist, 69, 1116–1126.

Allen, F.M. and Buseck, P.R. (1988) XRD, FTIR, and TEM studies of optically anisotropic grossularite garnets. American Mineralogist, 73, 568–584.

Akizuki, M. (1984) Origins of optical variations in grossular-andradite garnet. American Mineralogist, 69, 328–338.

Armbruster, T. and Geiger, C.A. (1993) Andradite crystal chemistry, dynamic X-site disorder and structural strain in silicate garnets. European Journal of Mineralogy, 5, 59–71.

Armbruster, T., Geiger, C.A., and Lager, G.A. (1992) Single-crystal X-ray structure study of synthetic pryope-almandine garnets at 100 and 293 K. American Mineralogist, 77, 512–521.

Artioli, G., Pavese, A., and Moze, O. (1996) Dispersion relations of acoustic phonons in pyrope garnet: relationship between vibrational properties and elastic constants. American Mineralogist, 81, 19–25.

Barker, F. (1964) Reaction between mafic magmas and pelitic schist, Cortlandt, New York. American Journal of Science, 262, 614–634.

Blanc, Y. and Maisonneuve, J. (1973) Sur la Birefringence des grenats calciques. Bulletin de la Societe Francaise de Mineralogie et de Cristallographie, 96, 320–321.

Bloss, F.D. (1971) "Crystallography and crystal chemistry", p. 432–433. Holt, Rinehart and Winston, New York.

Bosenick, A., Geiger, C.A., Schaller, T., and Sebald, A. (1995) A ^{29}Si MAS NMR and IR spectroscopic investigation of synthetic pyrope-grossularite garnet solid solutions. American Mineralogist, 80, 691–704.

Boyd, F.R. (1974) Ultramafic nodules from the Frank Smith Kimberlite pipe, South Africa. Carnegie Institution of Washington Yearbook, 73, 285–294.

Boyd, F.R. and Dawson, J.B. (1972) Kimberlite garnets and pyroxene-ilmenite intergrowths. Carnegie Institution of Washington Yearbook, 71, 373–384.

Brown, D. and Mason, R.A. (1994) An occurrence of sectored birefringence in almandine from the Gagnon Terrane, Labrador. Canadian Mineralogist, 32, 105–110.

Caporuscio, F.A. and Smyth, J.R. (1990) Trace element crystal chemistry of mantle eclogites. Contributions to Mineralogy and Petrology, 105, 550–561.

Chai, M. and Brown, J.M. (1997) The elastic constants of a pyrope-grossularite-almandine garnet to 20 GPa. Geophysical Research Letters, 24, 523–526.

Chase, A.B. and Lefever, R.A. (1960) Birefringence of synthetic garnets. American Mineralogist, 45, 1126–1129.

Chopin, C. (1984) Coesite and pure pyrope in high-grade blueschists of the Western Alps: a first record and some consequences. Contributions to Mineralogy and Petrology, 86, 107–118.

Deer, W.A., Howie, R.A., and Zussman, J. (1982) Rock Forming Minerals, vol. 1A: Orthosilicates, Longmans, London.

Dodge, F.C.W., Lockwood, J.P., and Calk, L.C. (1988) Fragments of the mantle and crust from beneath the Sierra Nevada batholith: Xenoliths in a volcanic pipe near Big Creek, California. Geological Society of America Bulletin, 100, 938–947.

Foord, E.E. and Mills, B.A. (1978) Biaxiality in 'isometric' and 'dimetric' crystals. American Mineralogist, 63, 316–325.

Ganguly, J., Cheng, W., O'Neill, H. St. C. (1993) Syntheses, volume, and structural changes of garnets in the pyrope-grossularite join: implication for stability and mixing properties. American Mineralogist, 78, 583–593.

Griffen, D.T. (1992) Garnet, p. 251–293. In "Silicate Crystal Chemistry," Oxford University Press, Oxford, U.K.

Griffen, D.T., Hatch, D.M., Phillips, W.R., and Kulaksiz, S. (1992) Crystal chemistry and symmetry of a birefringent tetragonal pyralspite$_{75}$-grandite$_{25}$ garnet. American Mineralogist, 77, 399–406.

Hietanen, A. (1963) Metamorphism of the Belt series in the Elk River-Clarkia area, Idaho. U.S. Geological Survey Professional Paper 344-C, 78 p.

Hofmeister, A.M. and Chopelas, A. (1991) Vibrational spectroscopy of end-member silicate garnets. Physics and Chemistry of Minerals, 17, 503–526.

Hofmeister, A.M., Fagan, T.J., Campbell, K.M., and Schaal, R.B. (1966) Single-crystal IR spectroscopy of pyrope-almandine garnets with minor amounts of Mn and Ca. American Mineralogist, 81, 418–423.

Ingerson, E. and Barksdale, J.D. (1943) Iridescent garnet from the Adelaide Mining District, Nevada. American Mineralogist, 28, 303–312.

Kano, H. and Yashima, R. (1976) Almandine-garnets of acid magmatic origin from Yamanogawa, Fukushima Prefecture and Kamitazawa, Yamagata Prefecture. Journal of the Japanese Association of Mineralogy, Petrology, and Economic Geology, 71, 106–119.

Kerr, P.F. (1977) Optical Mineralogy, 492 p. McGraw-Hill, New York.

Kingma, K.J. and Downs, J.W. (1989) Crystal-structure analysis of a birefringent andradite. American Mineralogist, 74, 1307–1316.

Kitamura, K. and Komatsu, H. (1978) Optical anisotropy associated with growth striation of yttrium garnet, $Y_3(Al,Fe)_5O_{12}$. Kristallographik Technik, 13, 811–816.

Koziol, A.M. and Newton, R.C. (1989) Grossular activity-composition relationships in ternary garnets determined by reversed displaced-equilibrium experiments. Contributions to Mineralogy and Petrology, 103, 423–433.

Lessing, P. and Standish, R.P. (1973) Zoned garnet from Crested Butte, Colorado. American Mineralogist, 58, 840–842.

Levin, S.B. (1950) Genesis of some Adirondack garnet deposits. Geological Society of America Bulletin, 61, 519–565.

Libowitzky, E. (1995) Optical anistropy of zoned magnetites due to form birefringence. Mineralogy and Petrology, 52, 107–111.

MacGregor, I.D. and Carter, J.L. (1970) The chemistry of clinopyroxenes and garnets of eclogite and peridotite xenoliths from the Roberts Victor Mine, South Africa. Physics of the Earth and Planetary Interiors, 3, 391–397.

MacGregor, I.D. and Manton, W.I. (1986) Roberts Victor eclogites: ancient oceanic crust. Journal of Geophysical Research, 91, 14063–14079.

McAloon, B.P. and Hofmeister, A.M. (1993) Single-crystal absorption and reflection infrared spectroscopy of birefringent grossularite-andradite garnets. American Mineralogist, 78, 957–967.

———(1995) Single-crystal IR spectroscopy of grossularite-andradite garnets. American Mineralogist, 80, 1145–1156.

McGetchin, R.T. and Silver, L.T. (1970) Compositional relations in minerals from kimberlite and related rocks in the Moses Rock Dike, San Juan County, Utah. American Mineralogist, 55, 1738–1771.

———(1972) A Crustal–Upper-Mantle Model for the Colorado Plateau Based on Observations of Crystalline Rock Fragments in the Moses Rock Dike. Journal of Geophysical Research, 77, 7022–7037.

McGetchin, R.T., Nikhanj, Y.S., and Chodos, A.A. (1973) Carbonatite-Kimberlite Relations in the Cane Valley Diatreme, San Juan County, Utah. Journal of Geophysical Research, 78, 1854–1869.

Meagher, E.P. (1982) Silicate garnets. In P.H. Ribbe, Ed., Orthosilicates, 5, 25–66.

Merli, M., Callegari, A., Cannillo, E., Caucia, F., Leona, M. Oberti, R., and Ungaretti, L. (1995) Crystal-chemical complexity in natural garnets: structural constraints on chemical variability. European Journal of Mineralogy, 7, 1239–1249.

Novak, G.A. and Gibbs, G.V. (1971) The crystal chemistry of the silicate garnets. American Mineralogist, 56, 791–825.

O'Neill, B., Bass, J.D., Smyth, J.R., and Vaughan, M.T. (1989) Elasticity of a grossularite-pyrope-almandine garnet. Journal of Geophysical Research, 94, 17819–17824.

Owen, J.V. and Marr, R A. (1990) Contrasting garnet parageneses in a composite Grenvillian granitoid pluton, Newfoundland. Mineralogical Magazine, 54, 367–380.

Pabst, A. (1936) Vesuvianite from Georgetown, California. American Mineralogist, 21, 1–10.

———(1943) Large and small garnets from Fort Wrangell, Alaska. American Mineralogist, 28, 233–245.

Prandl, W. (1966) Verfeinerung der Kristallstruktur des Grossulars mit Neutronen und Röntgenstrahlbeugung. Zeitschrift für Kristallographie, 123, 81–116.

Quartieri, S., Chaboy, J., Merli, M., Oberti, R., and Ungaretti, L. (1995) Local structural environment of calcium in garnets: a combined structure-refinement and XANES investigation. Physics and Chemistry of Minerals, 22, 159–169.

Rossman, G.R. and Aines, R.D. (1986) Birefringent garnet from Asbestos, Quebec, Canada. American Mineralogist, 71, 779–780.

Rossmanith, E. and Armbruster, T. (1995) The intensity of forbidden reflections of pyrope: Umweganregung or symmetry reduction? Zeitschrift für Kristallographie, 210, 645–649.

Schaal, R.B. (1991) I. Geometric modeling in reaction space of mineralogical diversity among eclogites, II. Constraints on shallow subduction of the Farallon plate from mantle xenoliths of the Colorado Plateau, 128 p. Ph.D. dissertation, University of California, Davis.

Smyth, J.R. and Hatton, C.J. (1977) A coesite-sanidine grospydite from the Roberts Victor kimberlite. Earth and Planetary Science Letters, 34, 284–288.

Smyth, J.R., Madel, R.E., McCormick, T.C., Munoz, J.L., and Rossman, G.R. (1990) Crystal structure refinement of a F-bearing spessartine garnet. American Mineralogist, 75, 314–318.

Sobolev, N.V., Kuznetsova, I.K., and Zyuzin, N.I. (1968) The petrology of grospydite xenoliths from the Zagadochnaya kimberlite pipe in Yakutia. Journal of Petrology, 9, 252–280.

Thompson, P.J. (1985) Stratigraphy, structure and metamorphism in the Moradnock quadrangle, New Hampshire. Contribution no. 58, Department of Geology and Geography, University of Massachusetts, Amherst, 191 p.

Ungaretti, L., Leona, M., Merli, M., and Oberti, R. (1995) Non-ideal solid-solution in garnet: crystal-structure evidence and modeling. European Journal of Mineralogy, 7, 1299–1312.

Zen, E. and Hammarstrom, J.M. (1988) Mineralogy and a petrogenetic model for the tonalite pluton at Bushy Point, Revillagigedo Island, Ketchikan 1° × 2° quadrangle, Southeastern Alaska. In K. Reed and Bartsch-Winkler, Eds., The U.S. Geological Survey in Alaska: Accomplishments during 1982. U.S. Geological Survey Circular no. 939, p. 118–123.